Nonlinear Dyn
https://doi.org/10.1007/s11071-018-4164-7

ORIGINAL PAPER

Stick-slip vibration of a cantilever beam subjected to harmonic base excitation

Hong-In Won · Booyeong Lee · Jintai Chung

Received: 3 August 2017 / Accepted: 19 February 2018

Abstract Stick-slip vibration of a cantilever beam subjected to harmonic base excitation is analyzed in this paper. To model the stick-slip vibration, considering nonlinearity and discontinuity of the friction force, two kinds of equations of motion are used: one for motion in the stick state and the other for motion in the slip state. Using the finite element method, dynamic responses of stick-slip vibration are calculated by iteratively solving the equations and connecting the stick- and slip-state motions; such calculations are conducted for various excitation conditions. The dynamic responses show that the occurrence of stick-slip vibration depends on excitation amplitude and frequency, and an occurrence of stick-slip vibration is associated with the modal characteristic of a beam. Furthermore, to formulate an analytical expression for the criterion of stick-slip occurrence, the static friction force caused by the base excitation is determined analytically. Finally, excitation conditions for stick-slip occurrence are obtained and validated in a parametric plane of the excitation amplitude and frequency, and design guidelines for avoiding stick-slip occurrence are presented.

H.-I. Won · B. Lee · J. Chung (✉)
Department of Mechanical Engineering, Hanyang University, 55, Hanyangdaehak-ro, Sangnok-gu, Ansan, Gyeonggi-do 15588, Republic of Korea
e-mail: jchung@hanyang.ac.kr

H.-I. Won
e-mail: luvhayym@hanyang.ac.kr

B. Lee
e-mail: lby87@hanyang.ac.kr

Keywords Stick-slip vibration · Nonlinearity and discontinuity of the friction force · Finite element method · Modal characteristic of a beam · Excitation conditions for stick-slip occurrence

1 Introduction

Stick-slip vibration is a repetitive motion between sticking and slipping of two contact surfaces. Many engineers are interested in stick-slip vibration because it produces unpleasant noise and vibrations in mechanical systems. For instance, in the automotive industry, it is well known that stick-slip vibration induces squeaking noises from vehicle interior components (such as door trim, cockpit modules, seat frames, and sunroof headliners); thus, suppressing stick-slip vibration is becoming a significant area of interest [1,2]. There is a growing sense among customers that the sound and vibration quality of machinery is of equal importance to mechanical performance, and this is leading to a demand for fundamental studies of stick-slip vibration.

Several researchers have attempted to understand stick-slip vibration using self-excited oscillator models. Some have reported nonlinear characteristics of friction force that lead to stick-slip vibration and have explained how to model stick-slip vibration [3–6]. Such researchers have made it clear that that stick-slip vibration arises from differences between static and kinetic forces and have introduced many friction models for numerical computation. Others have analyzed

Published online: 26 February 2018

the dynamic responses of stick-slip vibration numerically and experimentally and have tried to identify the main factor in the occurrence of stick-slip vibration [7–11]. These researchers reported that stick-slip vibration disappears when damping or sliding speed is increased and pointed out that the variation in kinetic friction force is an important factor in the occurrence of stick-slip vibration.

With the goal of improving practical systems that consist of several continuous parts, stick-slip vibration of continuous structures has also been investigated. Particularly, a great deal of research has been carried out on the stick-slip vibration of a continuous beam, because beam structures are fundamental components of mechanical systems that suffer from stick-slip vibration. For instance, transverse stick-slip vibration of a beam has been studied to examine mechanical noise and vibration problems in machine tools, robot legs, microscopy probes, and so on [12–18]. Stick-slip vibration of a beam in the torsional direction has been investigated for application to rotating beams such as propeller shafts and drill strings [19–23]. In these research efforts, the dynamic response and instability of stick-slip vibrations were analyzed in various manners, and then design guides and control methods to reduce stick-slip vibration were presented.

The present authors conducted a thorough literature search, finding many investigations by many researchers of the stick-slip vibration that occurs when a beam is translated or rotated in a certain direction with respect to the contact surface, as enumerated above. However, we found no theoretical study of the stick-slip vibration that occurs when the beam is oscillated by base excitation. This type of situation is quite important to designers attempting to analyze and suppress the unpleasant noise and risky vibration arising from stick-slip motion, generated from an assembled beam that is mounted on a vibratory structure or is subjected to transmitted force.

It is our carefully considered opinion that there is a lack of deep theoretical knowledge about stick-slip vibration of a beam with base excitation, because of a number of difficulties. First, it is difficult to model and analyze stick-slip vibration of a beam because the beam has different boundary conditions depending on its contact state. In other words, a beam must have a fixed boundary condition for the stick state and a friction force boundary condition for the slip state. In addition, because the boundary condition for the sticking motion with base excitation would be defined as a time-dependent boundary condition, it is difficult to solve the beam vibration analytically in order to calculate the static friction force initially acting on a beam in the stick state to cause stick-slip vibration to occur. Hence, overcoming these difficulties and then constructing and analyzing stick-slip vibration of a beam considering base excitation represents a new challenge that has not been previously accomplished.

Furthermore, study of the stick-slip vibration of a beam under base excitation can contribute to design guidelines for beam assembly modules to suppress stick-slip vibration problems. Even though the contact noise and vibration problems arising from stick-slip vibration of a beam have been matters of interest for a long time, it has still not been theoretically identified what conditions or circumstances lead to stick-slip vibration. In particular, in the automotive industry, stick-slip vibrations induced by vehicle interior modules made up of beam parts are becoming one of the most important issues in attempts to reduce vehicle operating noise and vibration and to develop electric vehicles. For this reason, analyzing the conditions in which stick-slip vibration occurs and suggesting design guidelines for beams to avoid stick-slip vibrations are worthwhile efforts that will be helpful to mechanical engineers.

Accordingly, the purpose of the present paper is to analyze nonlinear stick-slip vibration of a cantilever beam arising from harmonic base excitation and to present a criterion for the occurrence of stick-slip vibration. In Sect. 2, the contact state of the beam is classified into stick and slip states, and corresponding equations of motion and boundary conditions are derived. Transition conditions for both states are also discussed. In Sect. 3, vibration responses of the beam due to base excitation are calculated using the finite element method and the generalized-α time integration method [24], and the conditions leading to stick-slip vibration are investigated by studying various excitation frequencies and amplitudes. In Sect. 4, to analyze the criterion of stick-slip occurrence, an analytical response of the static friction force is theoretically derived when a beam is subjected to base excitation. Herein, a coordinate system for deflection of the beam is transformed through a quasi-static approach to allow an approximate solution to the time-dependent boundary condition problem. Finally, in Sect. 5, the magnitude of the analytical static friction force is compared with

the maximum static friction force in order to identify the excitation conditions leading to stick-slip vibration. The validity and usability of the presented results are verified through numerical simulations.

2 Equations for stick and slip states

This study considers a uniform and slender cantilever beam, mounted on a rigid base and in contact with a frictional wall (Fig. 1). The beam has length L, cross-sectional area A, area moment of area I, mass density ρ, and Young's modulus E. An axial force P is imposed at the rigid base and is propagated to the right end of the beam. Herein, it is assumed that the axial deformation is relatively small compared to the lateral deflection; thus, vibration in the axial direction is neglected. In this respect, based on the Euler–Bernoulli beam theory, the governing equation for the lateral deflection $u(x,t)$ can be expressed as follows:

$$\rho A\frac{\partial^2 u}{\partial t^2}+EI\frac{\partial^4 u}{\partial x^4}+P\frac{\partial^2 u}{\partial x^2}=-\rho A\frac{\partial^2 h}{\partial t^2}, \tag{1}$$

where t is time, x is the axial distance from the origin, and $h(t)$ represents a transverse displacement of the rigid base, which is determined as a function of time, by the excitation condition of the beam. Thus, transverse displacement of the beam denoted by $y(x,t)$ can be expressed as $y(x,t) = h(t) + u(x,t)$, as shown in Fig. 1.

The beam has two kinds of contact states, termed the stick and slip states. These terms refer to the sliding velocity relative to the frictional wall at the right end, $v_s = \partial y/\partial t|_{x=L}$, and boundary conditions of the beam are applied differently for each state. The stick state is the state in which the sliding velocity is zero ($v_s = 0$),

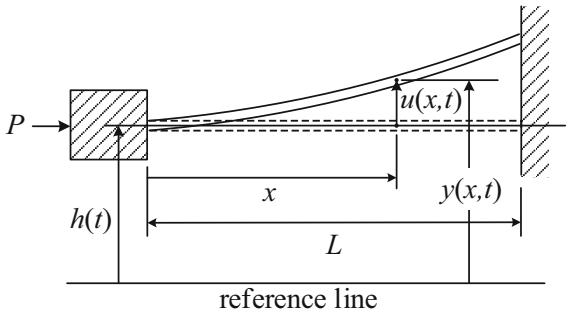

Fig. 1 Stick-slip vibration model of a cantilever beam mounted on a rigid base

meaning that the right end of the beam is stuck to the wall. The boundary conditions of the beam for the stick state can be defined as a clamped–pinned condition, expressed as follows:

$$u(x,t)=0,\quad u'(x,t)=0 \text{ at } x=0 \tag{2}$$

$$u(x,t)=u_s-\int_{t_s}^{t}\dot{h}(\tau)\mathrm{d}\tau,$$

$$EIu''(x,t)=0 \text{ at } x=L, \tag{3}$$

where u_s is a constant value for deflection at the right end of the beam, measured at the starting time of the stick state, which is denoted by t_s. The prime and dot marks are notations representing differentiations with respect to position x and time t, respectively. Equation (2) expresses the condition in which the deflection of the left end and its slope are zero. The first equation of (3) expresses the condition in which deflection at the right end is changing owing to the travel of the rigid base during the stick state, and the second equation of (3) means that the moment at the right end is zero; these boundary conditions were demonstrated by experimental testing.

In the stick state, a static friction force f_s arises between the beam and the wall as a reaction force corresponding to shear force at the right end; it cannot exceed the maximum static friction force. That is to say, the stick state can be maintained until the magnitude of the static friction force is less than the maximum static friction force. Thus, the necessary condition for the stick state to continue can be expressed as follows:

$$|f_s|=\left|EI\,u'''\right|_{x=L}\left|\leq\mu_s P,\right. \tag{4}$$

where μ_s is the coefficient of static friction. Equation (4) means that the magnitude of the static friction force is equal to the magnitude of the shear force at the right end and less than or equal to the maximum static friction force. Thus, when $|f_s|$ exceeds $\mu_s P$, the right end of the beam begins slipping, and the contact state of the beam changes from the stick state to the slip state.

On the other hand, the slip state occurs when the sliding velocity is not zero ($v_s \neq 0$), meaning that the beam is sliding on the frictional wall, and a kinetic friction force f_d is applied at the right end. In the slip state, the boundary conditions at the left end ($x = 0$) are same as those of the stick state given in (2). But because the position of the right end is not constrained on the wall, the boundary conditions at the right end ($x = L$) differ from those of the stick state and can be expressed as follows.

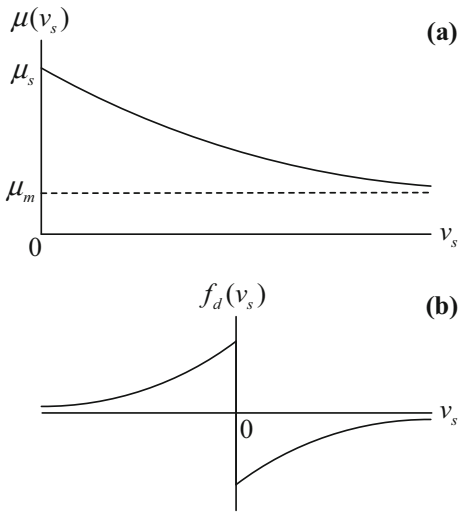

Fig. 2 Exponential-type friction model: **a** the friction coefficient versus the sliding velocity and **b** the friction force versus the sliding velocity

$$EIu''(x,t) = 0, \quad EIu'''(x,t) = -f_d \text{ at } x = L. \quad (5)$$

Equation (5) expresses the situation in which the moment at the right end is zero and the shear force at the right end is determined by the kinetic friction force. Because the kinetic friction force f_d acts in the direction opposite to the sliding velocity v_s,

$$f_d(v_s) = -\operatorname{sgn}(v_s)\mu(v_s)P, \quad (6)$$

where $\mu(v_s)$ is the kinetic friction coefficient, which is dependent on the sliding velocity v_s. In mechanical engineering, many kinds of friction models are used to determine the kinetic friction coefficient [4].

Among these, the present study used an exponential-type friction model [11] that is widely used to represent dry friction between solid surfaces. In the exponential-type friction model, the friction coefficient is initially equal to the maximum static friction coefficient μ_s. This coefficient gradually decays to the minimum kinetic coefficient μ_m when the magnitude of the sliding velocity $|v_s|$ is increased (Fig. 2a). The model can be mathematically expressed as follows:

$$\mu(v_s) = \mu_m + (\mu_s - \mu_m)\mathrm{e}^{-\alpha|v_s|}, \quad (7)$$

where α is a control parameter that determines the rate of decay of the kinetic friction coefficient. When the sliding velocity becomes zero again ($v_s = 0$) and the necessary condition for the stick state is satisfied, as given in (4), the beam's motion changes to the stick state. The kinetic friction force is obtained by multiplying the kinetic friction coefficient by the axial force P. The range of the static friction force is given by $-\mu_s P \le f_d \le \mu_s P$. Therefore, as shown in Fig. 2b, the friction force has a discontinuity at $v_s = 0$, which may lead to difficulties of a numerical method when computing dynamic responses for stick-slip vibration.

To establish a numerical analysis model for stick-slip vibration by the finite element method, variational equations for the stick and slip states are derived. Trial and weighting functions, respectively, denoted by $u(x,t)$ and $w(x,t)$, are defined as follows. The trial function u is a function that satisfies natural and geometric boundary conditions, as an approximate solution for the transverse deflection of the beam. The weighting function w is an arbitrary and infinitesimal function and is zero at a position where the geometric boundary conditions are specified. Because the boundary conditions at the right end of the beam depend on the stick and slip states, as expressed in Eqs. (3) and (5), the trial and weighting functions also depend on the two states, so separate variational equations are derived for the two states. First, by multiplying the weighting function w by the governing equation (1) and integrating the resulting equation from $x = 0$ to L and then applying the boundary conditions (2) and (3) by integration by parts, the following variational equation of the stick state can be obtained:

$$\int_0^L \left(\rho A w\ddot{u} + EIw''u'' - Pw'u'\right)\mathrm{d}x = -\int_0^L \rho A w\ddot{h}\mathrm{d}x. \quad (8)$$

Likewise, from the governing equation (1) and boundary conditions (2) and (5), the following variational equation of the slip state can be obtained:

$$\int_0^L \left(\rho A w\ddot{u} + EIw''u'' - Pw'u'\right)\mathrm{d}x = -\int_0^L \rho A w\ddot{h}\mathrm{d}x + w|_{x=L}\left(f - P\,u'\big|_{x=L}\right). \quad (9)$$

Next, the trial function $u(x,t)$ is separated into new variables $\bar{u}(x,t)$ and $\tilde{u}(x,t)$ to impose the geometric boundary conditions, in which $\bar{u}$ and $\tilde{u}$ are trial functions for active degrees and for specified geometric boundary conditions, respectively. By introducing $\bar{u}$ and $\tilde{u}$ into Eqs. (8) and (9), the variational equations of the stick and slip states can be rewritten respectively as follows:

$$\int_0^L \left(\rho A w\ddot{\bar{u}} + EIw''\bar{u}'' - Pw'\bar{u}'\right) \mathrm{d}x$$
$$= -\int_0^L \left[\rho A w(\ddot{h} + \ddot{\tilde{u}}) + EIw''\tilde{u}'' - Pw'\tilde{u}'\right] \mathrm{d}x \tag{10}$$

$$\int_0^L \left(\rho A w\ddot{\bar{u}} + EIw''\bar{u}'' - Pw'\bar{u}'\right) \mathrm{d}x$$
$$= w|_{x=L}\left(f - P\,\bar{u}'|_{x=L}\right)$$
$$-\int_0^L \left[\rho A w(\ddot{h} + \ddot{\tilde{u}}) + EIw''\tilde{u}'' - Pw'\tilde{u}'\right] \mathrm{d}x. \tag{11}$$

Lastly, by discretizing the variational equations into element matrix-vector equations and then assembling the resultant equations to give global matrix-vector equations, equations of motion for the stick and slip states are obtained, and a finite element model of the beam is finally established. In the present work, a two-node beam element is used for the finite element method.

3 Beam vibration due to harmonic excitation

It is interesting to study the vibration of the beam due to base excitation, because stick-slip vibration can occur depending on the conditions of the excitation. To calculate the vibration of the beam, at every moment, the contact state of the beam is first determined according to criterion conditions explained in Sect. 2, and then the equation of motion for the corresponding state is solved by the generalized-α time integration method [24] using the time step size of 10^{-4} s. This step size is chosen by trial and error to obtain reasonable computation results. For convenience of numerical computation, the criterion conditions for the sliding velocity $v_s = 0$ and $v_s \neq 0$ are changed to $|v_s| \leq \varepsilon$ and $|v_s| > \varepsilon$, respectively, where ε represents a threshold value for the sliding velocity that is sufficiently close to zero. The right end of the beam is considered to be in the stick state if the sliding velocity v_s is zero and the static friction force f_s is bounded by the maximum static friction force (i.e., $|v_s| \leq \varepsilon$ and $|f_s| \leq \mu_s P$). Otherwise, the stick state is switched to the slip state. The condition to switch between the stick and slip states is explained in [18] in more detail.

As the initial conditions, the deflection and velocity of the beam are set to zero, and the beam is stuck to the wall at $t = 0$. The sinusoidal function $A_0 \sin\Omega t$ is used to express the transverse displacement of the rigid base $h(t)$ as the harmonic base excitation, in which A_0 and Ω, respectively, denote the excitation amplitude and frequency. Unless otherwise noted, the following values of dimensions and material properties are used for the computer simulation: $L = 2\mathrm{m}$, $A = 0.01\mathrm{m}^2$, $I = (1/12) \times 10^{-6}\mathrm{m}^4$, $\rho = 1000\mathrm{kg/m}^3$, $E = 2 \times 10^9\mathrm{N/m}^2$, $P = 500\mathrm{N}$, $\mu_s = 0.6$, $\mu_m = 0.3$, $\alpha = 1$, and $\varepsilon = 10^{-4}\mathrm{m/s}$. Herein, the mass density ρ and Young's modulus E refer to the material properties of acrylonitrile butadiene styrene, a widely used engineering plastic, and the dimensions of the beam are selected to demonstrate the stick-slip vibration obviously and clearly.

To begin with, when the left end of the beam is excited with the fixed excitation amplitude $A_0 = 0.5\,\mathrm{mm}$, vibration responses of the beam are computed for various values of the excitation frequency $\Omega = 15$, 25, 35, and 70 Hz. The corresponding time flow motions and time histories of displacement at the right end of the beam are shown in Figs. 3 and 4, respectively. As shown in the figures, when the excitation frequency Ω is 15 Hz (Figs. 3a, 4a) or 35 Hz (Figs. 3c, 4c), the right end does not move and is stationary. In other words, the beam vibrates in the stick state at all times while the rigid base oscillates. However, when the excitation frequency Ω is 25 Hz (Figs. 3b, 4b) or 70 Hz (Figs. 3d, 4d), the right end moves from its original position, after which it repeatedly becomes stuck and moves again; that is to say, stick-slip vibration occurs. In these results, it is shown that stick-slip vibration occurs under 25 Hz excitation, but not the faster 35 Hz excitation.

As a next step, the excitation amplitude is increased to $A_0 = 1\,\mathrm{mm}$, and the vibration responses of the beam are computed with the same excitation frequencies given above; the corresponding time histories of displacement at the right end of the beam are plotted in Fig. 5. Under this amplitude, the beam remains in the stick state only at 15 Hz (Fig. 5a), and stick-slip vibration of various patterns occurs under excitations of 25, 35, and 70 Hz (Fig. 5b–d). In comparison with the cases of 0.5-mm excitation amplitude, stick-slip vibration additionally occurs at 35 Hz. It is considered natural that stick-slip vibration is more likely to occur as the excitation amplitude increases. However, because stick-slip vibration still does not occur at 15 Hz, it is interesting to determine the minimum excitation ampli-

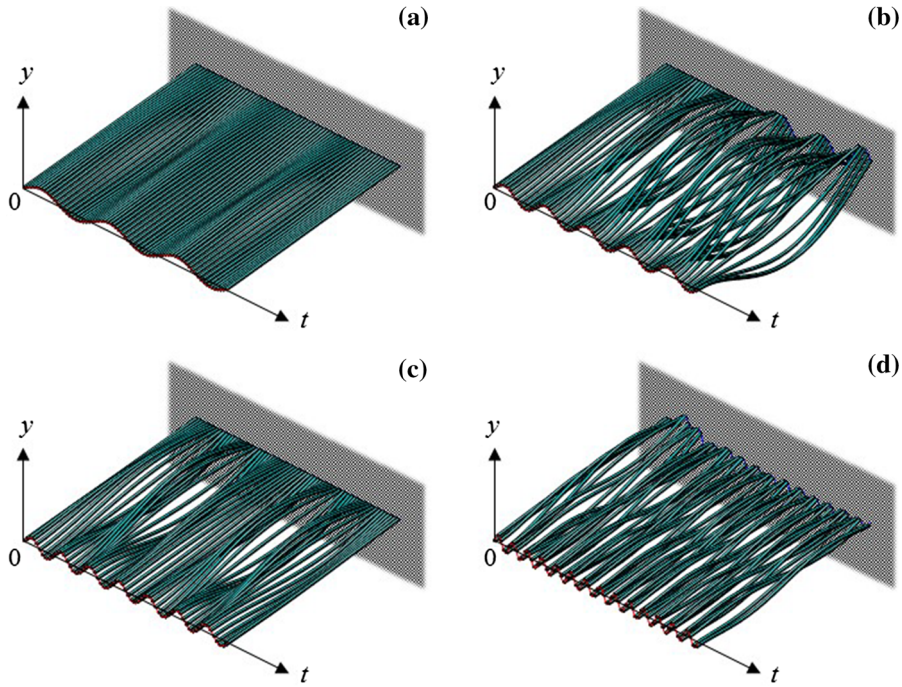

Fig. 3 Time flow motion of the beam for various excitation frequencies Ω of **a** 15, **b**, 25, **c** 35, and **d** 70 Hz at the oscillation amplitude A_0 of 0.5 mm

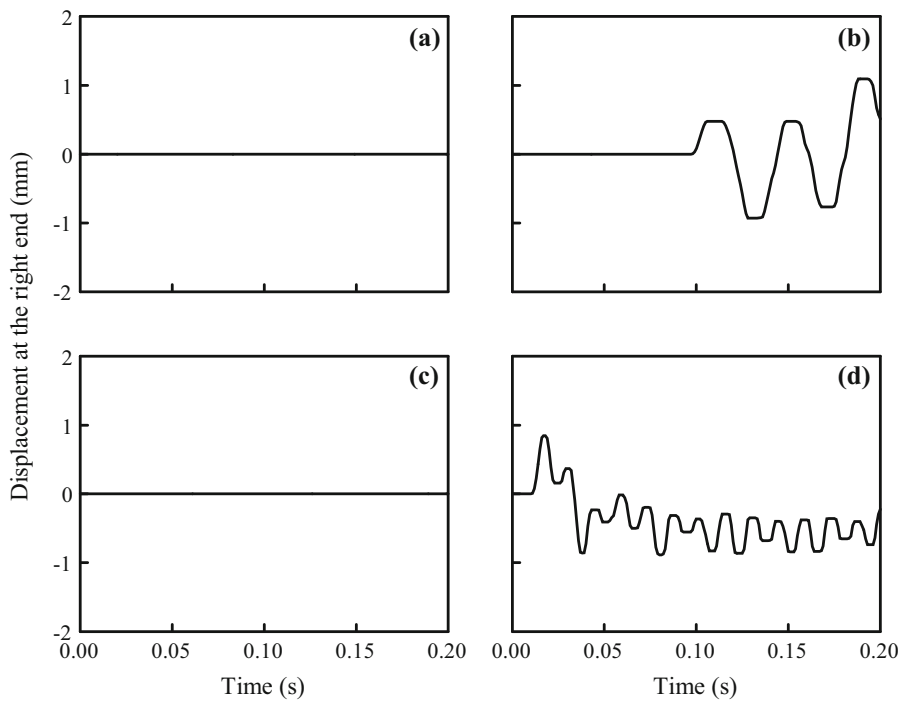

Fig. 4 Time histories of displacement at the right end for various excitation frequencies Ω of **a** 15, **b**, 25, **c** 35, and **d** 70 Hz at the oscillation amplitude A_0 of 0.5 mm

tude (i.e., the critical amplitude) required at a given frequency for stick-slip vibration to occur.

To investigate the critical amplitudes for various excitation frequencies, numerical simulations were carried out in which the excitation amplitude was iteratively increased from zero in increments of 0.01 mm until stick-slip motion was detected. In this way, for excitation frequencies from 5 to 100 Hz with the step

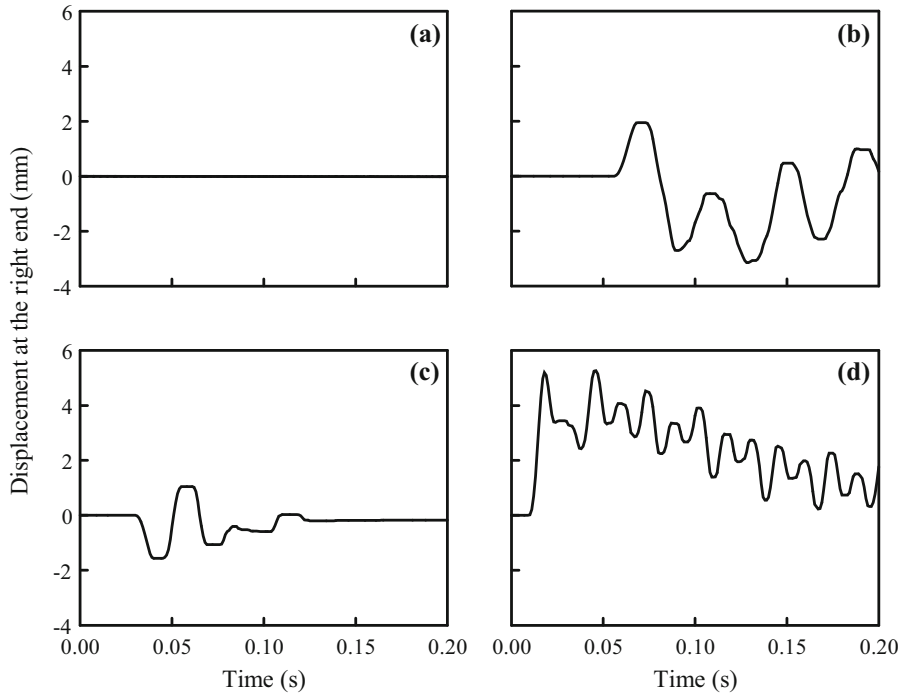

Fig. 5 Time histories of displacement at the right end for various excitation frequencies Ω of **a** 15, **b**, 25, **c** 35, and **d** 70 Hz at the oscillation amplitude A_0 of 1.0 mm

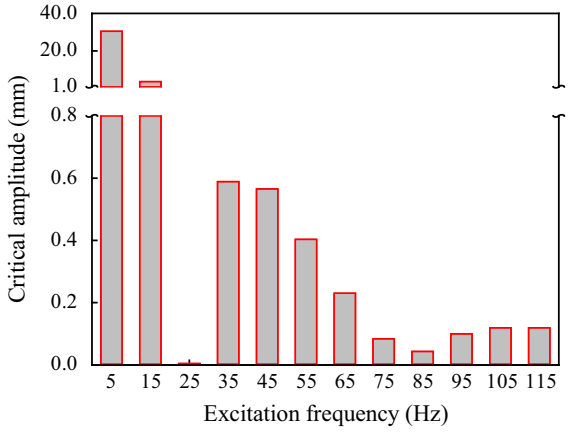

Fig. 6 Critical amplitudes of stick-slip occurrence for various excitation frequencies

size of 5 Hz, the critical amplitudes for stick-slip occurrence were obtained as drawn in Fig. 6. In addition, to facilitate understanding of the result, natural frequencies and mode shapes of the beam in the stick and slip states were calculated by performing modal analysis (Fig. 7). As shown in Fig. 6, the critical amplitude generally decreases with increasing excitation frequency, but is extremely small at 25 Hz and shows a slight valley at 85 Hz. This is because, as shown in Fig. 7, the excitation frequencies of 25 and 85 Hz are close to the first and second natural frequencies of the beam in the stick state, 25.0 and 81.1 Hz, respectively. In other words, because the beam vibrates in the stick state alone, if the excitation frequency is close to any natural frequency of the stick state, the beam vibration at the right end has small amplitudes.

4 Analytical expression for static friction force

It is valuable to obtain a criterion for the occurrence of stick-slip vibration in the form of analytical formulas, because this occurrence is difficult to predict due to the complex relations between the excitation conditions and the modal characteristics of the beam, as discussed above. Although this criterion can be obtained numerically as shown in Fig. 6, it is difficult to establish a numerical analysis model, and iterative simulations are very time-consuming. In this section, prior to obtaining a criterion for stick-slip occurrence, we first analytically derive the static friction force experienced at the right end of the beam.

As expressed in (4), because the static friction force corresponds to the reaction force of shear force at the right end of the beam in the stick state, a solution for the deflection of the beam in the stick state is first derived

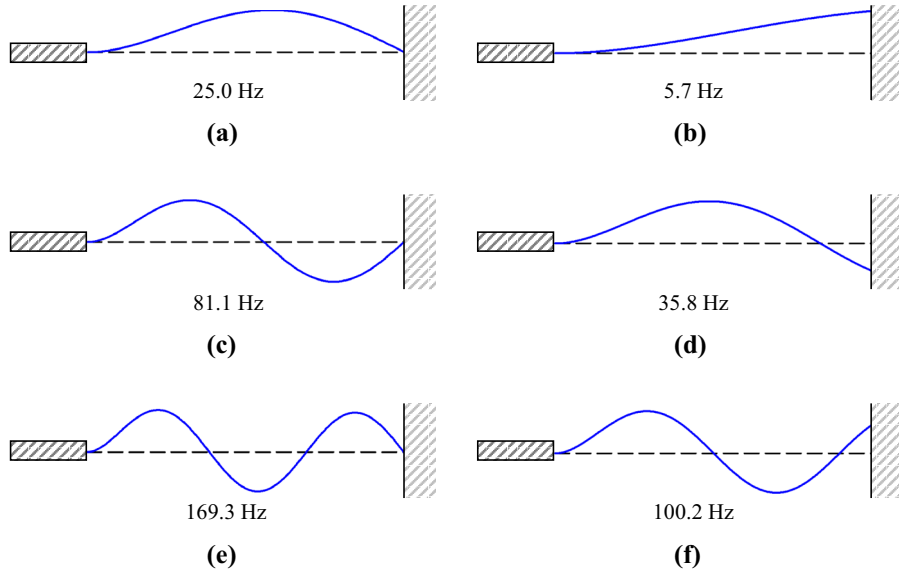

Fig. 7 Mode shapes and natural frequencies for the stick- and slip-state motions of the beam. **a** First mode in the stick state. **b** First mode in the slip state. **c** Second mode in the stick state. **d** Second mode in the slip state. **e** Third mode in the stick state. **f** Third mode in the slip state

using the governing equation (1) and the boundary conditions (2) and (3). Because the excitation function $A_0 \sin \Omega t$ is used as $h(t)$ and the beam begins to vibrate without any initial deflection, the geometric boundary condition at $x = L$ given in the first equation of (3) can be rewritten as $u(L, t) = -h(t) = -A_0 \sin \Omega t$. However, because this boundary condition is time dependent, the separation of variables, which is a well-known method for solving differential equations, cannot be used directly.

Thus, it is necessary to convert all boundary conditions to functions of only position, not time. Using the method proposed by Mindlin and Goodman [25], the variable u representing the deflection of the beam can be divided into two variables as follows.

$$u(x, t) = u_0(x, t) + \Delta u(x, t). \tag{12}$$

Herein, u_0 denotes the quasi-static deflection of the beam and Δu denotes the perturbed deflection of the beam measured from u_0 as illustrated schematically in Fig. 8. Assuming that u_0 is in the quasi-static state, substitution of (12) into (1) leads to the following two equations:

$$EI \frac{\partial^4 u_0}{\partial x^4} + P \frac{\partial^2 u_0}{\partial x^2} = 0 \tag{13}$$

$$\rho A \frac{\partial^2 \Delta u}{\partial t^2} + EI \frac{\partial^4 \Delta u}{\partial x^4} + P \frac{\partial^2 \Delta u}{\partial x^2} = -\rho A \left(\frac{\partial^2 h}{\partial t^2} + \frac{\partial^2 u_0}{\partial t^2} \right). \tag{14}$$

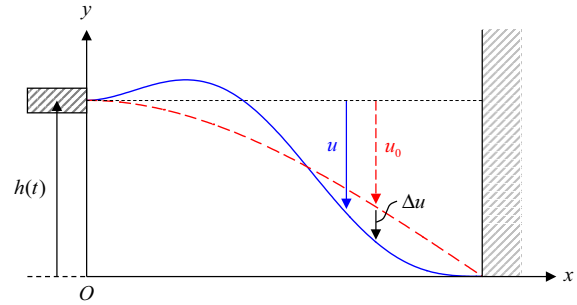

Fig. 8 Relation between coordinates of the beam: u is deflection measured from the base, u_0 is quasi-static-determined deformation, and Δu is perturbed deflection from u_0

Since the function u_0 should satisfy the time-independent boundary conditions, it can be expressed as

$$u_0(x, t) = S(x)h(t), \tag{15}$$

where $h(t)$ is given by $h(t) = A_0 \sin \Omega t$. Introducing (15) to (13), we obtain the following equation:

$$S^{(4)} + \sigma^2 S'' = 0, \tag{16}$$

where $\sigma = \sqrt{P/EI}$. When the rigid base has a unit displacement, the time-independent boundary conditions for (16) are given by

$$S(0) = 0, \quad S'(0) = 0, \quad S(L) = -1, \quad EIS''(L) = 0. \tag{17}$$

The solution of the governing equation (15) and the boundary conditions (17) can be obtained as

$$S(x) = \frac{-\sigma x \cos \sigma L + \sin \sigma L - \sin \sigma (L - x)}{\sigma L \cos \sigma L - \sin \sigma L}. \tag{18}$$

Next, a differential equation for Δu and its boundary conditions can be derived as follows:

$$\rho A\frac{\partial^2 \Delta u}{\partial t^2}+EI\frac{\partial^4 \Delta u}{\partial x^4}+P\frac{\partial^2 \Delta u}{\partial x^2} =-\rho A\frac{\partial^2 h}{\partial t^2}(1+S) \tag{19}$$

$$\Delta u(0,t)=0,\quad \frac{\partial \Delta u(0,t)}{\partial x}=0,\quad \Delta u(L,t)=0,$$
$$EI\frac{\partial^2 \Delta u(L,t)}{\partial x^2}=0. \tag{20}$$

As expressed in (20), all boundary conditions for Δu are time independent, so a solution for Δu can be approximated by applying the separation of variables method and the eigenmode expansion method as follows:

$$\Delta u(x,t)=\sum_{n=1}^{N} U_n(x)T_n(t), \tag{21}$$

where U_n is a basis function of the nth eigenmode, T_n is a modal coordinate of U_n, which is a function of time to be determined, and N is the total number of bases. In this study, $N = 10$ is used for analysis. The total number of bases is determined by some convergence tests for time responses. The basis function U_n satisfies the differential equation (19) and the boundary conditions (20) as an eigenfunction, written as

$$U_n(x)=\cosh\beta_n x-\cos\bar{\beta}_n x -\frac{\cosh\beta_n L-\cos\bar{\beta}_n L}{\bar{\beta}_n\sinh\beta_n L-\beta_n\sin\bar{\beta}_n L}\left(\bar{\beta}_n\sinh\beta_n x-\beta_n\sin\bar{\beta}_n x\right), \tag{22}$$

where β_n and $\bar{\beta}_n$ are the nth solutions of the following characteristic equation.

$$\beta\tan\bar{\beta}L=\bar{\beta}\tanh\beta L \text{ where } \beta^2,\bar{\beta}^2 =\frac{-P}{2EI}\pm\sqrt{\left(\frac{P}{2EI}\right)^2+\frac{\rho A\omega^2}{EI}} \tag{23}$$

in which ω is the natural frequency. When the axial force P is zero, (22) and (23) are, respectively, the same as the eigenfunction and characteristic equation for a clamped–pinned cantilever beam.

By substituting (21) into (19) and applying the orthogonal condition of eigenfunctions, the modal equations for T_n can be derived as N independent equations as follows:

$$\ddot{T}_n(t)+\omega_n T_n(t)=C_n\ddot{h}(t) \text{ for } n=1,2,\ldots,N \tag{24}$$

where ω_n is the natural frequency of the nth eigenmode and C_n is a generalized force coefficient for each modal equation. The natural frequency and generalized force coefficient, ω_n and C_n, can be expressed as follows:

$$\omega_n=\sqrt{\frac{\int_0^L\left(EIU_n''U_n''-PU_n'U_n'\right)\mathrm{d}x}{\int_0^L\rho AU_nU_n\mathrm{d}x}},$$
$$C_n=\frac{-\int_0^L U_n(1+S)\,\mathrm{d}x}{\int_0^L U_nU_n\mathrm{d}x}. \tag{25}$$

As expressed by (24), because each modal equation for T_n is equivalent to a single-degree-of-freedom mass–spring system, the forced vibration response for T_n can be solved using the convolution integral after replacing $h(t)$ with $A_0\sin\Omega t$. This yields the following solution for T_n:

$$T_n(t)=A_0\Omega^2C_n\left[\frac{-\Omega\sin\omega_n t+\omega_n\sin\Omega t}{(\Omega^2-\omega_n^2)\omega_n}\right]. \tag{26}$$

By collecting the above equations and according to the relation given in (12), an approximate solution for deflection of the beam subjected to harmonic base excitation can be expressed as follows:

$$u(x,t)=A_0\left\{S(x)\sin\Omega t+\sum_{n=1}^{N}U_n(x)\Omega^2C_n\left[\frac{-\Omega\sin\omega_n t+\omega_n\sin\Omega t}{(\Omega^2-\omega_n^2)\omega_n}\right]\right\}. \tag{27}$$

Finally, the following expression is obtained for the response of the static friction force between the beam and the wall due to the base excitation:

$$f(t)=EI\left.\frac{\partial^3 u}{\partial x^3}\right|_{x=L} =EIA_0\left\{\left.\frac{\partial^3 S}{\partial x^3}\right|_{x=L}\sin\Omega t+\sum_{n=1}^{N}\left.\frac{\partial^3 U_n}{\partial x^3}\right|_{x=L}\Omega^2C_n\left[\frac{-\Omega\sin\omega_n t+\omega_n\sin\Omega t}{(\Omega^2-\omega_n^2)\omega_n}\right]\right\}. \tag{28}$$

According to (28), the response of the static friction force $f(t)$ is proportional to the flexural rigidity of the beam EI and the excitation amplitude A_0. We can also see from the form of this equation that resonance occurs and the static friction force is drastically amplified as the excitation frequency Ω approaches any natural frequency of the beam ω_n because the denominator $(\Omega^2-\omega_n^2)\omega_n$ of the last term of (28) approaches zero in this situation.

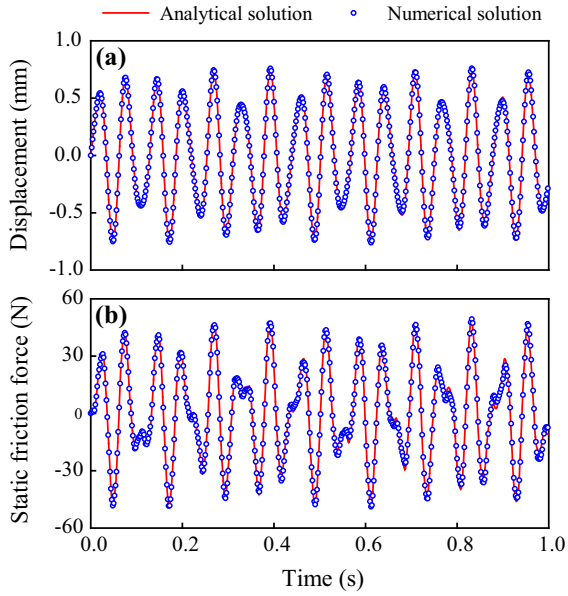

Fig. 9 Comparison of **a** displacement at $x = 0.5L$ and **b** the static friction force for the excitation amplitude and frequency of $A_0 = 0.5\,\text{mm}$ and $\Omega = 15\,\text{Hz}$

Solutions for the deflection of the beam and the response of the static friction force analytically obtained by applying (27) and (28) were verified by comparison with solutions numerically calculated by applying the finite element model established in Sect. 2. The conditions used were $A_0 = 0.5\,\text{mm}$ and $\Omega = 15\,\text{Hz}$, with other parameters being the same as given in Sect. 3. Figure 9a shows the time response of the displacement of the beam measured at $x = 0.5L$; i.e., $y(0.5L,t) = h(t) + u(0.5L,t)$, and Fig. 9b shows the time response of the static friction force $f(t)$. In each plot, the solid line represents the analytical solution and the circle symbols represent the numerical result. The analytical solutions obtained by applying (27) and (28) fit very well with the numerical results, validating the accuracy and usefulness of the presented analytical method.

5 Criterion of stick-slip occurrence

The analytical expression of static friction force obtained above allows us to predict which excitation conditions can lead to stick-slip vibration. Because stick-slip vibration occurs when the static friction force exceeds the maximum static friction force, the criterion for stick-slip occurrence can be defined as follows:

$$\text{If } |f_{\max}| \le \mu_s P, \text{ stick-slip vibration cannot occur .} \tag{29}$$

$$\text{If } |f_{\max}| > \mu_s P, \text{ stick-slip vibration can occur .} \tag{30}$$

Herein, $|f_{\max}|$ denotes the absolute maximum of the static friction force while the beam is subjected to base excitation, calculated according to (28) under the assumption that the beam vibrates in the stick state. Basically, if the maximum static friction force exceeds $\mu_s P$, slipping will occur, leading to stick-slip vibration; otherwise, the beam will remain in the stick state.

To determine the excitation conditions that are expected to result in stick-slip vibration according to (29) and (30), the absolute maximum of the static friction force $|f_{\max}|$ can be calculated for given base excitation amplitude and frequency. Unfortunately, because the response of the static friction force as expressed in (28) is of complex and nonlinear form with respect to time, it is difficult to obtain $|f_{\max}|$ in a closed-form equation. Thus, in the present work, the response of the static friction force is calculated over the time range from 0 to 10 s, and $|f_{\max}|$ is considered to be the maximum absolute value of the results. The absolute maxima of the static friction force $|f_{\max}|$ obtained in this manner over the range of excitation amplitudes from 0 to 1 mm and the range of excitation frequencies from 0 to 120 Hz are plotted in Fig. 10; the other parameters used are as given in Sect. 3. In addition, the maximum static friction force $\mu_s P = 300\,\text{N}$ is drawn in the figure as a flat plane. The absolute maximum of the static friction force $|f_{\max}|$ seems to increase generally with increasing excitation amplitude or frequency, but is sharply amplified and shows a resonance effect for excitation frequencies close to the natural frequencies of the stick state ω_n.

The results of using (28) to determine whether stick-slip occurs or not were compared with the responses obtained in Sect. 3. When the excitation amplitude A_0 is 0.5 mm, the excitation frequencies Ω of 15 and 35 Hz, respectively, result in $|f_{\max}|$ of 40.38 N (marked as A in Fig. 10) and 254.87 N (marked as B); both of which are less than $\mu_s P = 300\,\text{N}$. Thus, these excitation conditions can be determined to cause the stick state only. Contrastingly, the excitation frequencies of 25 and 70 Hz result in $|f_{\max}|$ of 3.03×10^4 N (marked as C) and 977.54 N (marked as D), which are greater

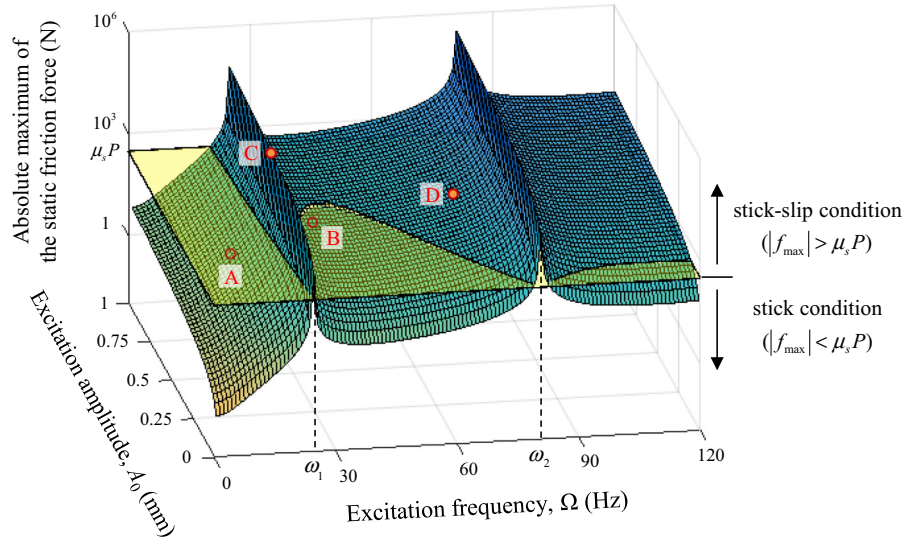

Fig. 10 Absolute maximum of the static friction force $|f_{\max}|$ versus base excitation amplitude and frequency compared to the maximum static friction force $\mu_s P$ (flat plane)

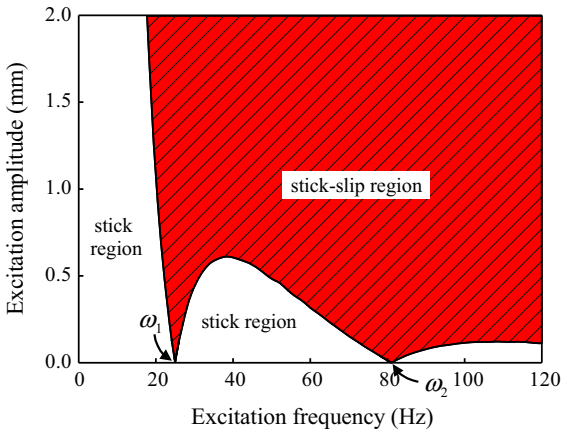

Fig. 11 Criterion diagram for stick-slip occurrence in the parametric plane of base excitation amplitude and frequency

than $\mu_s P = 300\,\mathrm{N}$, so that these excitation conditions can be determined to cause stick-slip vibration. The stick-slip occurrence results determined in this manner are consistent with those that were numerically investigated by the finite element model, explained in Figs. 3 and 4.

Furthermore, the excitation conditions for the stick-slip occurrence can also be represented using a parametric plane of base excitation amplitude and frequency as shown in Fig. 11, by tracking the excitation amplitude that satisfies $|f_{\max}| = \mu_s P$ at each excitation frequency. In this figure, the solid line indicates the excitation conditions of $|f_{\max}| = \mu_s P$ and the ω_1 and ω_2, respectively, indicate the first and second natural frequencies. Hence, the lower region represents the parametric area for the stick condition ($|f_{\max}| \leq \mu_s P$), i.e., the stick region, and the upper region represents the parametric area for the stick-slip condition ($|f_{\max}| > \mu_s P$), i.e., the stick-slip region. Figure 11 clearly shows that extremely small amplitudes are sufficient to produce stick-slip vibration when the excitation frequency is the same as the natural frequency of the stick state.

To validate the excitation conditions presented above for stick-slip occurrence, numerical simulations were performed using the finite element model developed in Sect 2 with respect to excitation conditions. The results appear in Fig. 12, overlaid on Fig. 11 trace of critical amplitudes. In the figure, the squares indicate the conditions of excitation amplitude and frequency that make the beam vibrate only in the stick state, and the circles indicate the conditions that lead to stick-slip vibration. The solid line represents the critical amplitude determined according to the analytical method (Fig. 11). As shown in the figure, the analytical and numerical solutions for the stick-slip occurrence agreed well. These results demonstrate that the analytical method presented herein can be used to predict the stick-slip occurrence, instead of time-consuming numerical simulations.

We now discuss how the stick-slip criterion is affected by decreases in the flexural rigidity of the beam. Related to this discussion, we performed calculations for the case in which the flexural rigidity of the beam EI is halved and the other parameters are unchanged compared to those used in the work

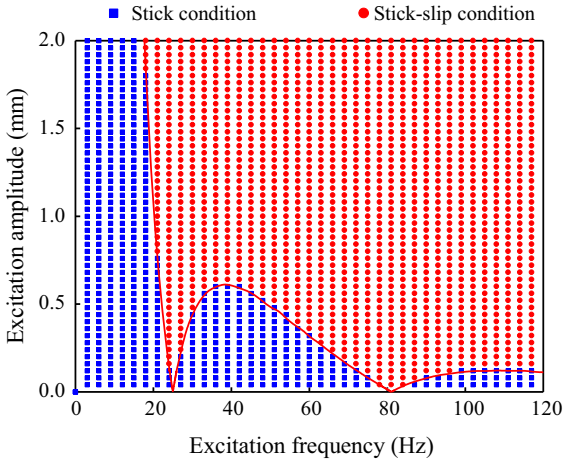

Fig. 12 Criterion diagram for stick-slip occurrence obtained by numerical simulations

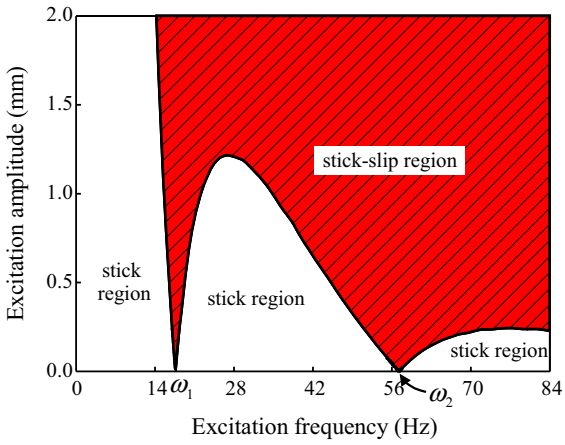

Fig. 13 Criterion diagram for stick-slip occurrence when the flexural rigidity *EI* is halved compared to the Fig. 11 case

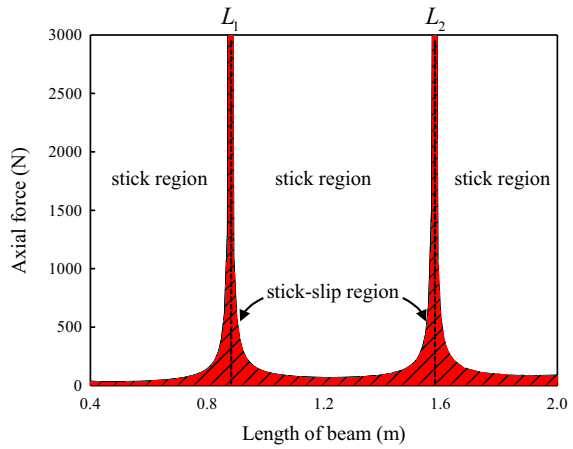

Fig. 14 Criterion diagram for stick-slip occurrence in the parametric plane of axial force P and beam length L for the fixed excitation amplitude and frequency of $A_0 = 1\,\text{mm}$ and $\Omega = 25\,\text{Hz}$, respectively

described above. In this case, the first three natural frequencies of the beam in the stick state were calculated as 17.6, 57.3, and 119.6 Hz, smaller than those of the previous case (25.0, 81.1, and 169.3 Hz). Accordingly, the excitation frequencies leading to resonance also decreased. By using the proposed method, the stick-slip criterion can be plotted as in Fig. 13. Because the frequency regions near the resonance frequencies, at which only small excitation amplitudes are required for stick-slip occurrence, differed from the previous case, the scale of the excitation frequency in Fig. 13 is adjusted for better comparison; as a result, the positions of the resonance frequencies appear equal to those of Fig. 11. Compared to Fig. 11, in Fig. 13, it can be seen that the critical amplitude for stick-slip occurrence is larger. In other words, a low-rigidity beam better withstands excitation and resists stick-slip vibration than a more rigid beam.

It is also interesting that the presented method can be used to determine design guidelines of a beam that will avoid stick-slip vibration. For example, when the excitation amplitude and frequency that a beam is subjected to are given by $A_0 = 1\,\text{mm}$ and $\Omega = 25\,\text{Hz}$, respectively, a diagram of the stick-slip criterion with respect to the beam length L and the axial force P can be obtained as shown in Fig. 14. In this case, the range of beam lengths considered is from 0.4 to 2 m, and the width and height of the beam are, respectively, set to 0.2 and 0.02 m, to satisfy Euler–Bernoulli beam theory, while the length of beam is varied. The other parameters, except axial force, are the same as before. In Fig. 14, the solid line corresponds to $|f_{\max}| = \mu_s P$, and the lower and upper regions represent the stick-slip region ($|f_{\max}| > \mu_s P$) and the stick region ($|f_{\max}| \leq \mu_s P$), respectively. The axial force must be extremely high to escape the stick-slip region when the length of the beam is close to L_1 and L_2. This is because the excitation frequency $\Omega = 25\,\text{Hz}$ coincides with the first natural frequency of the beam in the stick state when $L_1 = 0.88\,\text{m}$ and with the second natural frequency when $L_2 = 1.58\,\text{m}$. Thus, the occurrence of stick-slip vibration is inevitable in the vicinity of L_1 and L_2 under the given conditions, so a beam length

can be recommended by excluding values close to L_1 or L_2.

6 Conclusions

Stick-slip vibration of a cantilever beam under harmonic base excitation was studied herein. Variational equations of motion for the stick and slip states were respectively derived, considering the nonlinearity and discontinuity of the friction force with respect to the relative sliding velocity. Then, a numerical analysis model was established by means of the finite element method and the generalized-α time integration method. Using the numerical analysis model, vibration responses of the beam were investigated with respect to excitation amplitude and frequency. It was found that stick-slip vibration tends to occur as the excitation amplitude is increased or as the excitation frequency approaches the natural frequency of the beam in the stick
state.

Next, an analytical expression of static friction force was proposed. By this expression, a criterion for stick-slip occurrence was presented and validated. To determine this criterion, the response of the static friction force arising from the base excitation was theoretically derived. To solve the time-dependent boundary condition problem, the variable representing deflection of the beam was separated into two variables to allow a quasi-static approximation. Then, by comparing the analytical expression of static friction force with the maximum static friction force, a criterion of stick-slip occurrence was formulated with respect to the base excitation amplitude and frequency and was validated by comparison with the numerical results. By applying the proposed method, it was shown that a beam of lower flexural rigidity is more stable, resisting the occurrence of stick-slip vibration in terms of the normalized excitation frequency. In addition, we identified trends in beam length that can be recommended for avoiding stick-slip vibration as an example of an application to structural design. The proposed analytical approach to the criterion of stick-slip occurrence can be extended to various types of structures in addition to the beam and can be used to prevent the stick-slip vibration in many machines.

References

1. Shin, S.H., Cheong, C.: Experimental characterization of instrument panel buzz, squeak, and rattle (BSR) in a vehicle. Appl. Acoust. **71**, 1162–1168 (2010)
2. Trapp, M., Chen, F.: Automotive Buzz, Squeak and Rattle: Mechanisms, Analysis, Evaluation and Prevention. Elsevier, Amsterdam (2011)
3. Haessig, D.A., Friedland, B.: On the modeling and simulation of friction. Am. Contr. Conf. 1256–1261 (1990)
4. Berger, E.: Friction modeling for dynamic system simulation. Appl. Mech. Rev. **55**, 535–577 (2002)
5. Marton, L., Lantos, B.: Modeling, identification, and compensation of stick-slip friction. IEEE Trans. Ind. Electron. **54**, 511–521 (2007)
6. Leine, R.I., Van Campen, D.H., De Kraker, A.: Stick-slip vibrations induced by alternate friction models. Nonlinear Dyn. **16**, 41–54 (1998)
7. Popp, K., Stelter, P.: Stick-slip vibrations and chaos. Philos. Trans. R. Soc. A **332**, 89–105 (1990)
8. Ding, W., Shichao, F., Mingwan, L.: A new criterion for occurrence of stick-slip motion in drive mechanism. Acta Mech. Sin. **16**, 273–281 (2000)
9. Awrejcewicz, J., Dzyubak, L., Grebogi, C.: Estimation of chaotic and regular (stick-slip and slip-slip) oscillations exhibited by coupled oscillators with dry friction. Nonlinear Dyn. **42**, 383–394 (2005)
10. Pilipchuck, V., Olejnik, P., Awrejcewicz, J.: Transient friction-induced vibrations in a 2-DOF model of brakes. J. Sound Vib. **344**, 297–312 (2015)
11. Won, H.I., Chung, J.: Stick-slip vibration of an oscillator with damping. Nonlinear Dyn. **86**, 257–267 (2016)
12. Stelter, P.: Nonlinear vibrations of structures induced by dry friction. Nonlinear Dyn. **3**, 329–345 (1992)
13. Meziane, A., Baillet, L., Laulagnet, B.: Experimental and numerical investigation of friction-induced vibration of a beam-on-beam in contact with friction. Appl. Acoust. **71**, 843–853 (2010)
14. Saha, A., Pandey, S.S., Bhattacharya, B., Wahi, P.: Analysis and control of friction-induced oscillations in a continuous system. J. Vib. Control **18**, 467–480 (2012)
15. Seo, Y., Yabuno, H., Kono, G.: Mode coupling-type instability of a beam subjected to coulomb friction. J. Vib. Acoust. **135**, 064502 (2013)
16. Eigoli, A.K., Vossoughi, G.: Dynamic modeling of stick-slip motion in a legged, piezoelectric driven microrobot. Int. J. Adv. Robot Syst. **7**, 201–208 (2010)
17. Zhang, H., Zhang, S.Y., Fan, L.: Effects of stick-slip motions on Besocke-style scanners in scanning probe microscopes. J. Phys. D. Appl. Phys. **45**, 035303 (2011)
18. Won, H.I., Chung, J.: Numerical analysis for the stick-slip vibration of a transversely moving beam in contact with a frictional wall. J. Sound Vib. **419**, 42–62 (2018)
19. Khulief, Y.A., Al-Sulaiman, F.A., Bashmal, S.: Vibration analysis of drillstrings with self-excited stick-slip oscillations. J. Sound Vib. **299**, 540–557 (2007)
20. Liu, X., Vlajic, N., Long, X., Meng, G., Balachandran, B.: Nonlinear motions of a flexible rotor with a drill bit: stick-slip and delay effects. Nonlinear Dyn. **72**, 61–77 (2013)

21. Zhang, Z., Chen, F., Zhang, Z., Hua, H.: Analysis of friction-induced vibration in a propeller-shaft system with consideration of bearing-shaft friction. P. I. Mech. Eng. C-J. Mech. **228**, 1311–1328 (2014)
22. Qui, H., Yang, J., Butt, S.: Stick-slip analysis of a drill string subjected to deterministic excitation and stochastic excitation. Shock Vib. **2016**, 9168747 (2016)
23. Monteiro, H.L.S., Trindade, M.A.: Performance analysis of proportional-integral feedback control for the reduction of stick-slip-induced torsional vibrations in oil well drillstrings. J. Sound Vib. **398**, 28–38 (2017)
24. Chung, J., Hulbert, G.M.: A time integration algorithm for structural dynamics with improved numerical dissipation: the generalized-α method. J. Appl. Mech. Trans. ASME **60**, 371–375 (1993)
25. Mindlin, R.D., Goodman, L.E.: Beam vibrations with time dependent boundary conditions. J. Appl. Mech. Trans. ASME **17**, 377–380 (1950)